Bioorganic Chemistry 131 (2023) 106280

Contents lists available at ScienceDirect

Bioorganic Chemistry

journal homepage: www.elsevier.com/locate/bioorg

Synthesis, pharmacological evaluation, DFT calculation, and theoretical investigation of spirocyclohexane derivatives

Atef M. Abdel Hamid [a], Asmaa H. Amer [a], Mohamed G. Assy [a], Wael A. Zordok [a], Samar M. Mouneir [b], Samar El-Kalyoubi [c], Wesam S. Shehab [a,*]

[a] Department of Chemistry, Faculty of Science, Zagazig University, Zagazig 44519, Egypt
[b] Department of Pharmacology, Faculty of Veterinary Medicine, Cairo University, Cairo 12211, Egypt
[c] Department of Pharmaceutical Organic Chemistry, Faculty of Pharmacy (Girls), Al-Azhar University, Nasr City, Cairo 11651, Egypt

ARTICLE INFO

Keywords:
Spiro compounds
DFT
B3LYP HOMO - LUMO anti-inflammatory

ABSTRACT

Polycyclic structures fused at a central carbon are of great interest due to their appealing conformational features and their structural implications in biological systems. Although progress in the development of synthetic methodologies toward such structures has been impressive, the stereo selective construction of such quaternary stereo centers remains a significant challenge in the total synthesis of natural products. From the computational calculations by Density Functional Theory along with the B3LYP as basis set, It is obvious that the all studied compounds are soft molecules and η varied from 0.069 for compound (10) to 0.087 for compound (15), while the compound (14) is treated as hard molecule, the value of η is 0.102, also the electronic transition within the soft compounds is easy as indicated from the △E, the compound (10) is absolute soft according to the (σ = 14.49 eV), while the compound (14) is treated as hard compounds (σ = 9.804 eV). The newly formed compounds exhibited both anti-inflammatory and antioxidant activities on HRBC homolytic and membrane stabilization and DPPH scavenging percent, respectively.

1. Introduction

Spiro heterocycles have important applications in drug industry [1]. Spiro heterocyclic structure is a unique feature of several natural and synthetic products that possess remarkable biological activities [2–4]. The potential use of spiro heterocycles in medicinal chemistry has been well documented owing to their prominent pharmacological properties [5–11], and geochemistry [12–14]. Recently, several piperidine derivatives along with the incorporation of hetero conjugate groups at the nitrogen atom of the piperidine ring have been well explored by spectroscopic and X-ray analysis [15,16]. Earlier reports disclosed that with the blocking of a secondary nitrogen atom in the piperidine ring by electron donating or withdrawing groups, abrupt changes were observed in the ring conformations. the molecule displays different conformations such as a chair, boat, or twist-boat forms. One of the heterocycles, pyrrole, is not naturally derived, but its analogs are present in co-factors and natural products such as vitamin B_{12}, bile pigments: bilirubin and biliverdin [17–22]. Apart from this, pyrrole and pyrrolidine analogs have diverse therapeutic applications like fungicides, antibiotics, anti-inflammatory drugs, cholesterol-reducing drugs, antitubercular, and antitumor agents [23,24]. These are also known to inhibit reverse transcriptase in the case of human immune deficiency virus type 1 (HIV-1) and cellular DNA polymerase protein kinases [25,26]. The combination of different pharmacophores in a pyrrole and pyrrolidine ring system has led to more active compounds [27–32]. Therefore, the development of new spiroheterocycles having thiadiazol ring is worthwhile from the perspective of medicinal and material chemistry [33,34]. Increasing interest has been reported towards the biological activities of pyrrole and pyrrole derivatives [35–37]. The drugs containing pyrrole ring exert various pharmacological effects such as antipsychotic [38], anti-inflammatory [39,40], analgesic, antidepressant [41], antihypertensive [42], antimicrobial [43,44], anticonvulsant [45,46], antineoplastic [47,48], etc. Pyrroles and pyrrole derivatives contain an active hydrogen atom (N—H) and exhibit proven antioxidant activity [49–52]. The main goal of the research reported here was to synthesize and characterize spiro heterocyclic compounds and to estimate of the energies of these molecules which is very important both in theoretical studies and their chemical reactivity.

* Corresponding author.

https://doi.org/10.1016/j.bioorg.2022.106280
Received 27 September 2022; Received in revised form 5 November 2022; Accepted 13 November 2022
Available online 19 November 2022

2. Results and Discussions:

Spiro derivative **3** was prepared quantitatively by reacting an equimolar amount of primary amine at room temperature. The reaction may be started via cyan acetylation, followed by intramolecular cyclization to furnish the major compound **4** (Scheme 1). Spectroscopic analysis of **4**show NH and CO stretching signal at 3278 $cm^{-1}$and 1649 cm^{-1} respectively. The D_2O exchangeable signals for NH_2, NH were located at δ 8.10 ppm and δ 8.09 ppm, and the enaminic CH was shown at 3.56 ppm. cyclic enaminone **4**undergoes (3_+ 3) cycloaddition with benzylicto phenone via the formation of Michael adduct **6**, that cyclized intramolecularly providing pyridine derivative 7 (Scheme1).

IR of compound **7** leads to peaks at 3301 $cm^{-1}$and 1677 cm^{-1} for NH, C═O respectively. The acidic NH signal was detected at δ 8.11 ppm in ^{1}H NMR. In addition to aromatic protons and cyclic sp^3 protons. Moreover, The C═O and C═N carbon signals were located around δ 192 ppm and δ 162 ppm in ^{13}C NMR.

Reactive enaminic carbon of **3** undergoes addition of a molecule of benzaldehyde forming compound **9** followed by cyclization with loss of a molecule of NH_3 forming condensed pyrolopyridine derivative **10** (Scheme 2). IR of **10** revealed peaks at 3350 cm^{-1}, 1647 cm^{-1}, and 1605 cm^{-1} due to NH, C═O, and C═N (due to the tautomeric form of compound 10); respectively.

Acidic NH signal in ^{1}H NMR was observed at δ 8.23 ppm, and δ 8.25 ppm: respectively. Two carbon signals of the desired compound **10** were detected at δ 161.44 ppm, δ 161.36 ppm for C═O carbon.

Compound **4** condensed with the more reactive site of ninhydrin via the departure of H_2O followed by the addition of enaminic NH_2 to carbonyl function leading to poly heterocyclic **11**. IR of **11** contained OH, NH, and C═O. The OH involved in the hydrogen bond leads to a downfield signal in ^{1}H NMR at δ 10.52 ppm while aliphatic OH is located at δ 3.85 ppm. in ^{13}C NMR carbon signals appeared C═O at δ 167.26 and δ 168.50 ppm (Scheme 2).

Pyrrole derivative **4** underwent addition of an enaminic function to the polarized double bond of maleic anhydride tofurnish**15** (Scheme 3).

Stretching peaks for the product revealed OH and C═O at 3277 cm^{-1},1648 cm^{-1}respectively. NMR study provides OH and pyrrole-CH at δ 8.10 ppm, and δ 8.08 ppm, respectively.

As depicted in (Scheme4) compound **4** underwent1,4 additions to Acyl isothiocyanate to produce pyrimidine cyclization. Cyclic enaminone **4** was added to heteroallene electrophilic carbon, followed by intramolecular cyclodehydration forming condensed pyrimidines **18a, b**. The NH signals were detected in the region δ 9.52– 9.85 ppm. compound **18a** condensed with urea to form cyclic urea **19**. The, NH's, NH_2 signals were detected at δ 11.23 ppm, δ 9.85 ppm, and δ 9.55 ppm.

Compound **4**condensed with an equimolar amount of benzaldehydeto furnish α, β unsaturated cyclic compound **10.** The condensed pyridine **10** reacts with two molecular amounts of hydrazine. The reaction may be started via ring opening formic non-isolable acyclic hydrazide **21** followed by intramolecular cyclocondensationvia losing NH_3 and subsequent oxidation.Thechemical structure of **23**was provedby the presence of NH and carbonyl groups at 3293 $cm^{-1}$and 1647 cm^1 in IR and NH signalet δ 8.37 ppm (Scheme 5).

The condensed pyridine **10** undergo cyclocondensation with two molecular amounts of acetylacetone providing an enamine system **24** followed by condensation with exocyclic carbonyl resulting in a polycyclic system **25** (Scheme 6). Compound **25** showed absorption peaks at 3278 cm^{-1} for NH and 1640 cm^{-1} for α, β unsaturated carbonyl in IR spectra. Also, in ^{1}H NMR, the same compound provides signals at δ 8.10 ppm, δ 7.30–7.25 ppm for olefinic protons. upon treatment, the target **10** resulted in ring transformation yielding polyheterocyclic.

2.1. Structural parameters and models

2.1.1. Compound (7) 2′,4′-Diphenyl-3′,4′-dihydrospiro[cyclohexane-1,7′-pyrrolo[3,4-b] pyridin]-5′(6′H)-one (7)

The molecule is slightly sterically hindered, the atoms of this compound are distributed in the three planes as shown in Fig. 1. Thecyclohexane ring of the spiro ring system is lying in a perpendicular plane respected to the remaining part of the spiro ring system, the dihedral angles N20-C21-C23-C27 and N20-C21-C24-C25 are 69.54° and −69.61°, these values confirm that the two rings of spiro system are lying in the two perpendicular planes. Also, the dihedral angles C6-C21-C23-C27 and C6-C21-C24-C25 are 178.28° and −178.64°, while the pyrazole ring of the spiro group and pyridine ring are completely planers, the dihedral angles, C4-N5-C6-C21 and C1-*C*2-C19-N20 are 175.04° and −175.49°, also the dihedral angles N5-C6-C21-C24 and N5-C6-C21-C23 are −65.09° and 61.62°, these values confirm that the pyridine ring is lying in the same plane of pyrazole ring of spiro system and lying in perpendicular plane respect to the cyclohexane ring of spiro system. There is a plane occupied by the first phenyl ring and the pyridine ring, the dihedral angles N5-C4-C13-C14 and N5-C4-C13-C15 are −2.651° ≈ 0.00° and 176.98° ≈ 180.00°, also the dihedral angles C3-C4-C13-C15 and C3-C4-C13-C14 are 0.178° ≈ 0.00° and −179.46° ≈ 180.00°. While the second phenyl ring is lying in another plane occupied by the pyridine ring, the dihedral angles, *C*2-C1-C7-C12 and *C*2-C1-C7-C8 are 40.65° and

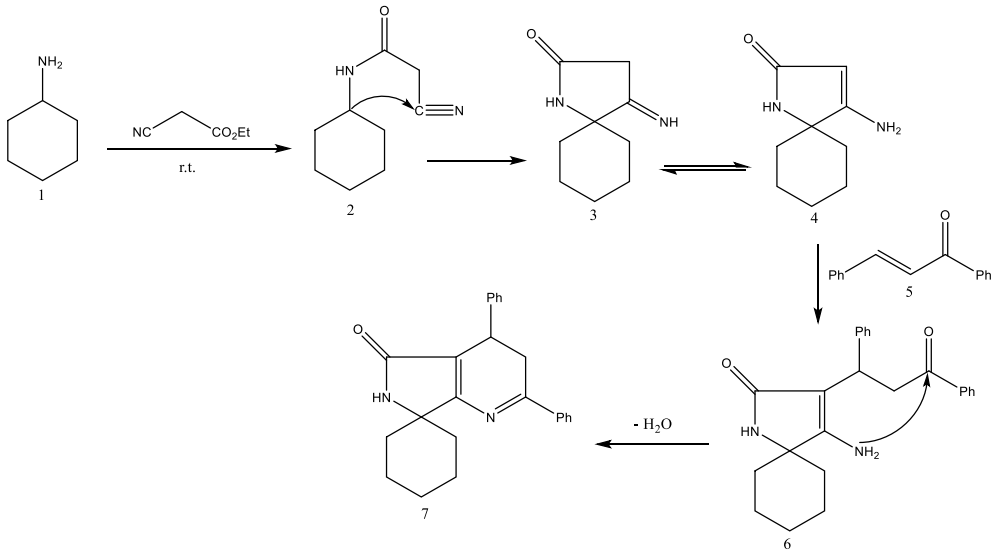

Scheme 1. Synthesis of spiro compound4 and cycloaddition of 4 with chalcone5.

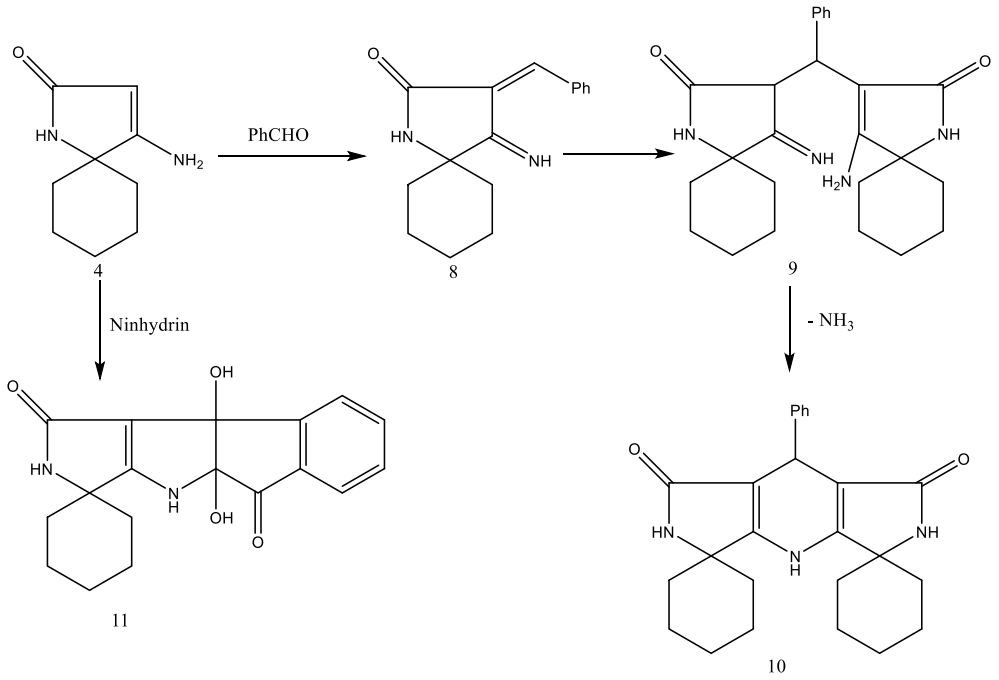

Scheme 2. Novel synthesis of condensed pyrroles 10 and 11.

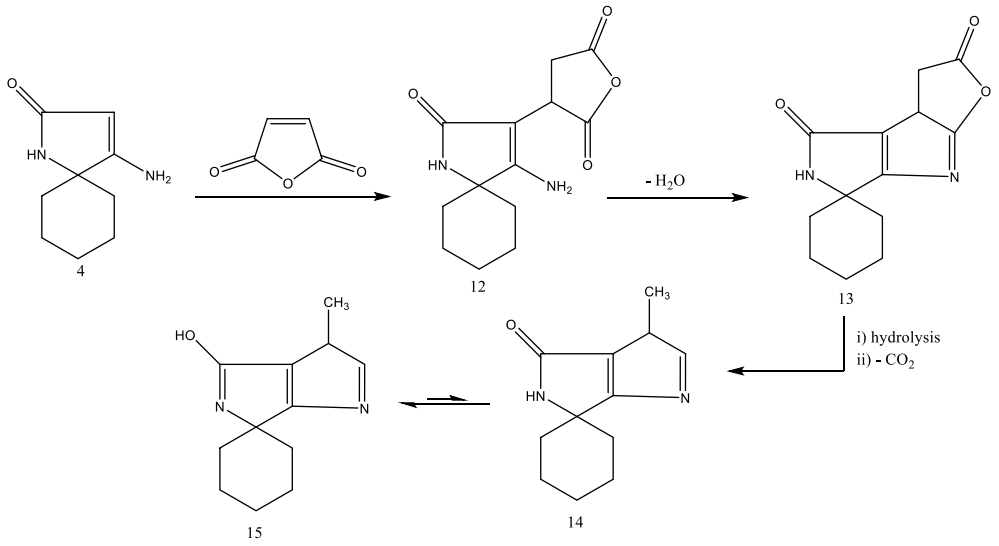

Scheme 3. Condensation of spiro pyrrole 4 with maleic anhydride.

−141.37°, while the dihedral angles, C3-C1-C7-C8 and C3-C1-C7-C12 are 100.16° and −77.82°, these values confirmed that the second phenyl ring is lying in perpendicular plane respect to the plane occupied by the pyridine ring and pyrazole ring of spiro system as seen in Fig. 1.

The C═O group attached directly through C19 of the spiro system, the bond angle C21C19O22 is 119.68° ≈ 120°, also all bond angles in this compound are varied from 106.38° for C2C1C3 to 136.37° for C1C2C9, these values reflect that the type of sp2 hybridization spreading over most atoms of the molecule, all bond angles, and dihedral angles are listed in **Table S1**. The non-planarity of the molecule playsan important role in its activity and biological activity, phenyl rings can be rotated around the carbon–carbon bonds, C4-C13 for the first phenyl ring and C1-C7 for the second phenyl ring. The value of the energy of this compound is −16760.368 kcal/mol and the presence of strong withdrawing groups as –C═O group besides other strong donating nitrogen atoms as N5 and N20 causes the generation of weak dipole moment 5.54D. The all-bond lengths in the two phenyl groups varied between 1.341 and 1.346 Å[58]and are the shortest C—C bonds in the whole molecule. The N5-C6 and C4-N5 bond lengths are 1.261 and 1.268 Å[56] are significantly shorter than the C19-N20 and N20-C21 bond lengths of 1.361 and 1.462 Å[57], there is a single bond character between N20 and C19 atoms and between N20 and C21 atoms [60], the bond lengths between nitrogen atom N5 and the neighbor carbon atoms C4 and C6 of the pyridine ring have double bond characters [61]. The bond lengths between atoms are listed in **Table S1**, these values are compared nicely with the crystal structure of the molecule has a similar structure [62]. Detailed analysis of corresponding bond lengths in various heterocyclic compounds was given elsewhere [63–66]. All distances and angles between the atoms of the ligand are given in **Table S1**.

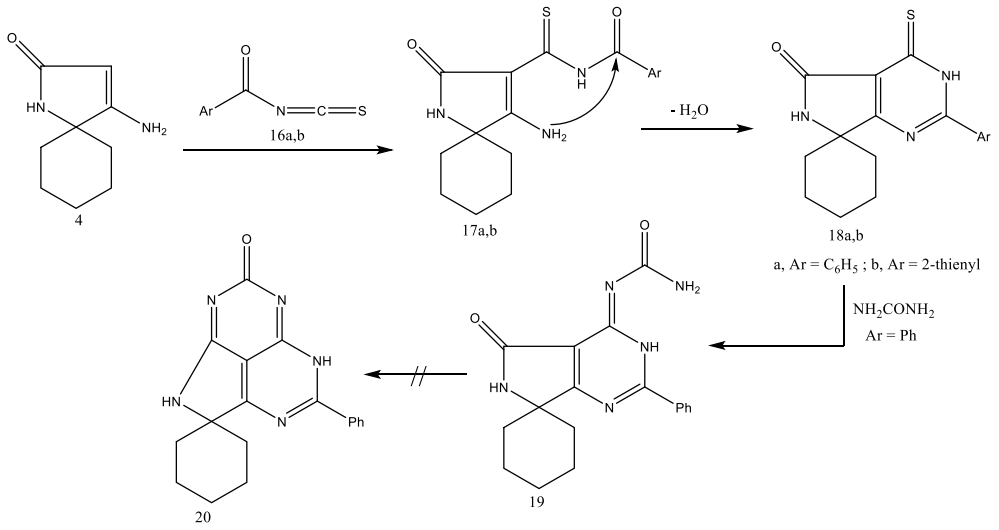

Scheme 4. Heterocyclization of spiro pyrrole 4 with aroyl isothiocyanates.

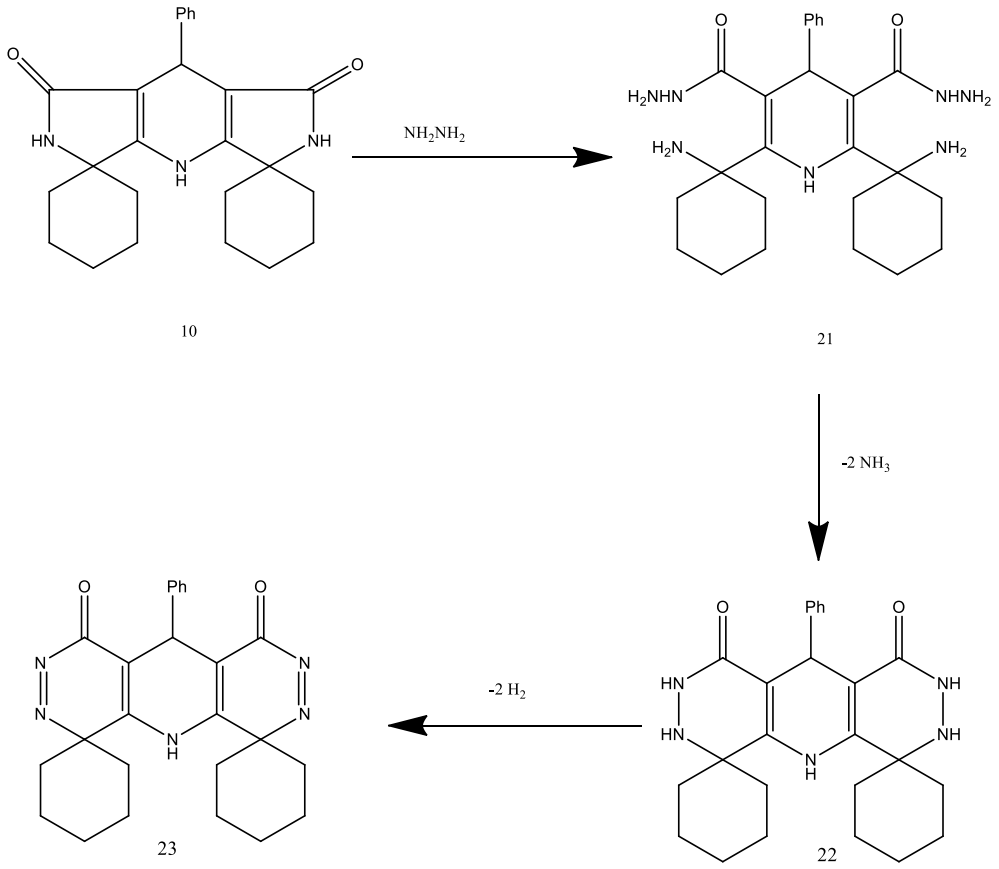

Scheme 5. Synthetic route of tricyclic compound 23.

2.1.2. Compound (10) 8′-Phenyl-4′,8′-dihydrodispiro[cyclohexane-1,3′-dipyrrolo[3,4-b:3′,4′-e] pyridine-5′,1′′-cyclohexane]-1′,7′(2′H,6′H)-dione

Fig. 2 shows the optimized geometrical structures of the compounds (10). The molecule is nonplanar, the non-planarityis attributed to the presence of two spiro systems fused through the central pyridine ring. All bond lengths of this compound are like the bond lengths of compound (**7**).

The dihedral angle of this compound as C1-*C*2-C13-N14 is 179.89°, while the dihedral angles N14-C15-C6-N5and N23-C24-C4-N5 are 179.19° and −176.89° ≈ 180°, respectively, also the dihedral angles C6-N5-C4-C24 and C15-C6-N5-C4 are −160.56° and 160.11°, respectively, these values confirmed that pyrazole rings of the two spiro systems and central pyridine ring are lying in the same plane. The dihedral angles C17-C15-N14-C13 and C3-C4-C24-C25 are −116.17° and 115.93°, respectively, these values confirmed that the two terminal rings of the two spiro systems are lying out of the plane occupied by the two pyrazole rings and central pyridine ring. Also, the dihedral angles C12-C7-C1-*C*2 and C12-C7-C1-C3 are 51.81° and −64.81°, these values reflect that the phenyl ring is lying in a perpendicular plane occupied by the central fused aromatic system consisting of the two pyrazole rings of the two

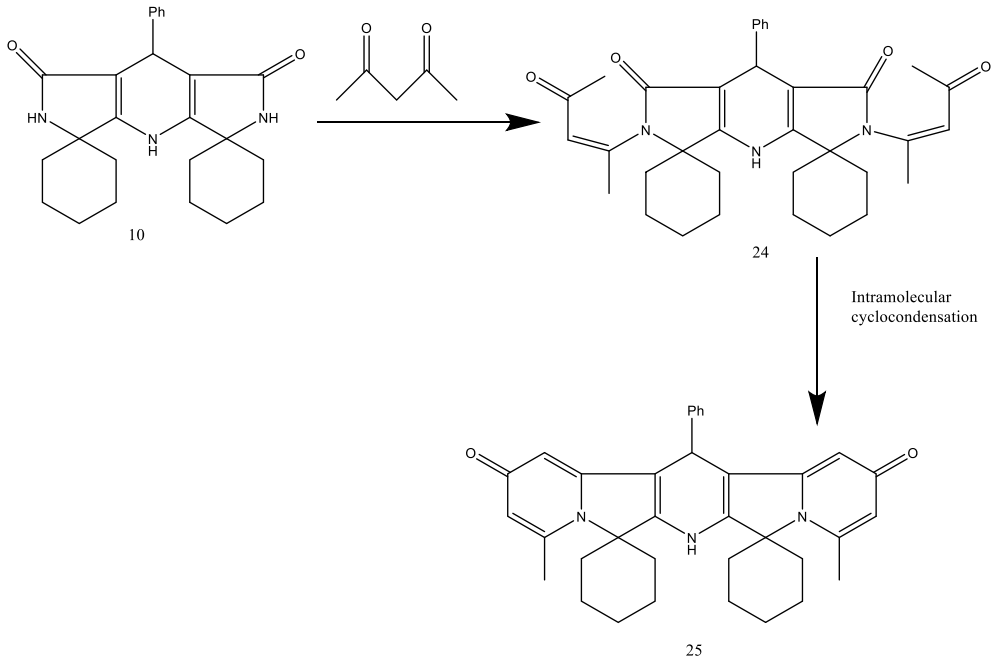

Scheme 6. Synthetic route of poly heterocyclic compound 25.

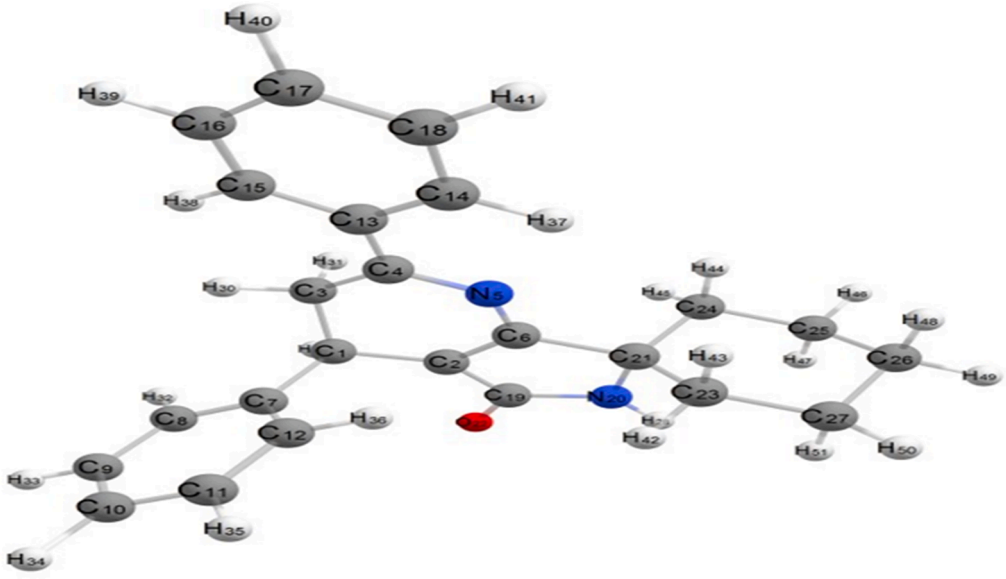

Fig. 1. Optimized geometrical structure of compound (**7**) by using DFT calculations.

spiro systems and the central pyridine ring. The value of bond angles around the carbon atoms in this compound varied between (110.38° for C7-C1-C3 and 134.67° for the C1-*C*2-C13 bond angle). Also, the angles around the nitrogen atoms of the two terminal pyrazole rings of the two spiro systems in the compound are varied between (127.28° and 129.42°), also the bond angle around nitrogen atom N5 of the central pyridine ring is 125.67°, these values reflect that the type of sp2 hybridization spreading over most atoms of this compound. The energy of the compound (**10**) has a more negative value of −18733.94 kcal/mol less than that of the energy of compound (**7**), the energy difference between this compound and compound (**7**) is ≈ 2000 kcal/mol, so the compound (**10**) is considered as more stable than compound (**7**). The presence of two spiro systems containing two strong withdrawing carbonyl groups have the same direction causing producing a greater dipole moment of 12.389D, this value is greater than the dipole moment of the compound (**7**). There is no large difference between the bond lengths between atoms in compound (**10**) and compound (**7**), the bond lengths between carbon atoms of the two terminal cyclohexane rings of the two spiro systems are varied from 1.533 to 1.536 [67] Å is the longest C—C bond in the whole molecule [68]. The bond distances between nitrogen atoms and neighboring carbon atoms are varied between 1.344 and 1.461 Å, respectively [69], whereas these bonds have a single bond character [70], there isa single bond character between N and C atoms [71]. The all-bond lengths, bond angles, and dihedral angles are listed in **Table S2**.

2.1.3. Compound (11) 4a',9b'-Dihydroxy-4',4a'-dihydrospiro [cyclohexane-1,3'-indeno[2,1-b] pyrrolo[3,4-d] pyrrole]-1',5'(2'H,9b'H)-dione

show the optimized geometrical structures of the compound (11), this compound is like compound (**10**) in all parameters and structures

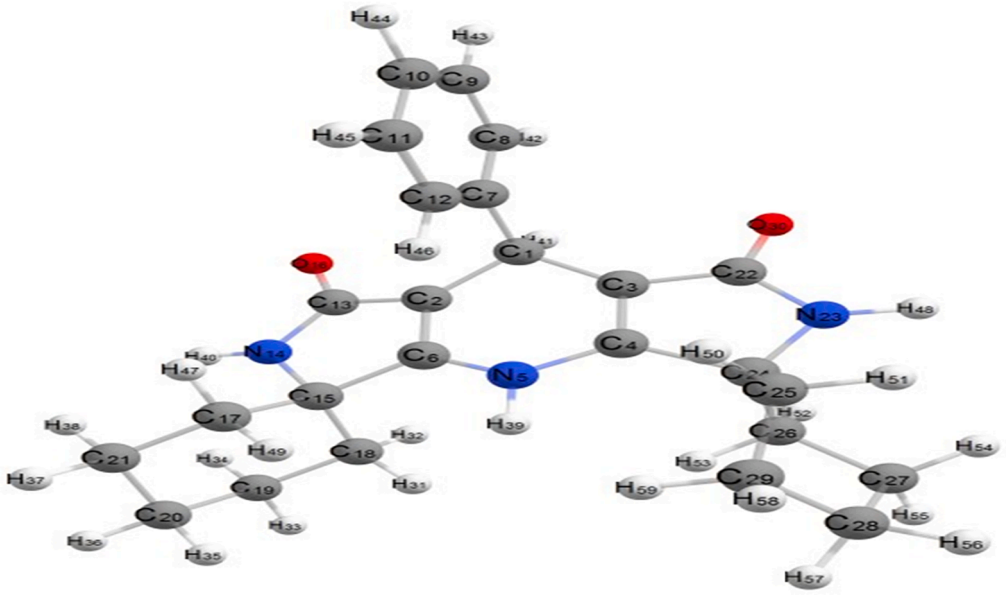

Fig. 2. Optimized geometrical structure of compound (10) by using DFT calculations.

with the replacement of with replacing of one spiro system by indigo system. The energy of the compound (**11**) has a higher value of −13402.747 kcal/mol, this value greater than that of the energy of compound (**10**) by 5000 kcal/mol and higher than the energy of compound (**7**) by 3000 kcal/mol. All parameters of this compound are given in **Table S3**. The presence of two C═O groups have opposite directions as shown in Fig. 3 causing a lowering of the value of dipole moments, the value of dipole moment is 4.763D, this value is lower than both compounds (**7**) and (**10**).

2.1.4. Compound (14) 3′-Methyl-3′H-spiro[cyclohexane-1,6′-pyrrolo[3,4-b] pyrrol]-4′-ol

The optimized geometrical structures of the compounds (14) is shown in Fig. 4**,** this compound has the different structure features of the compound (1) although they have similar composition with replacement of pyridine ring in compound (1) by pyrole ring in compound (4), the cyclohexane ring of spiro system is lying out of the plane occupied by the fused aromatic system. The two fused pyrole rings are lying in the same plane, the dihedral angle N1-C5-C8-N4 is 178.65°, all dihedral angles between atoms in the fused system are nearly from 0.00° or 180.00°. But the dihedral angles C11-C8-C5-C1 and C11-C8-C5-N4 are 116.34° and −63.19°, these values reflect that the cyclohexane ring of spiro system is lying in perpendicular plane respect to the fused aromatic system of the two fused pyrole rings. Also, the methyl group is lying out the plane occupied by the central fused aromatic system, the dihedral angleC15-C2-C3-N4 is 169.41°. The energy of this compound, −9405.289 k cal/mol is higher than the energy of compound (1), also the value of dipole moment, 2.689D less than compound (7). All geometrical parameters as bond lengths, bond angles and dihedral angles are given in **Table S4**.

2.1.5. Compound (15) 3′-methyl-3′H-spiro[cyclohexane-1,6′-pyrrolo[3,4-b] pyrrol]-4′-ol

The optimized geometrical structures of the compounds (**15**) are shown in Fig. 5,

The presence of the –OH group causes rising in the total energy value by ≈ 1.00 kcal/mol. The presence of the –OH group attached to the pyrrole ring causes a lowering of the value of dipole moment, 2.298D. All these values are listed in **Table S5**.

2.1.6. Compound (19) 7-methyl-2H-spiro[2,3,5,6,8-pentaazaacenaphthylene-1,1′-cyclohexan]-4(6H)-one

Fig. 5 shows the optimized geometrical structures of the compound

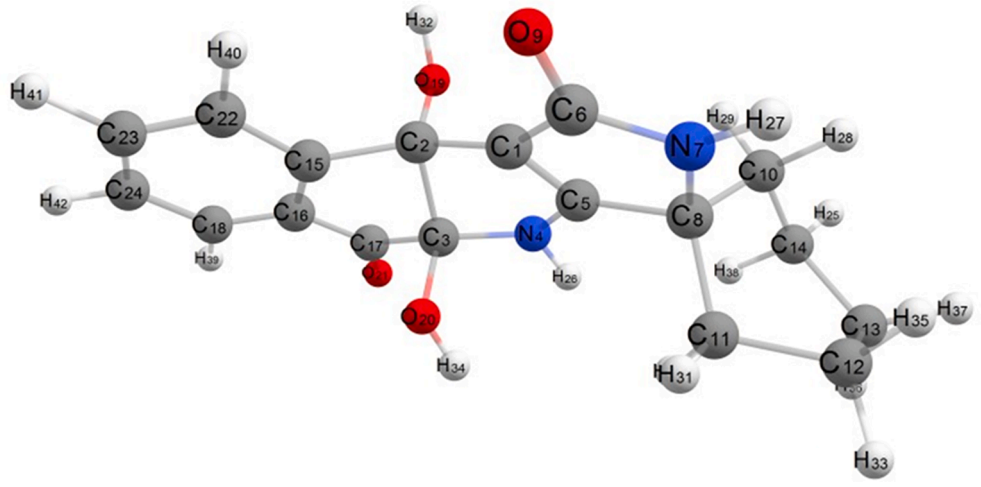

Fig. 3. Optimized geometrical structure of compound (11) by using DFT calculations.

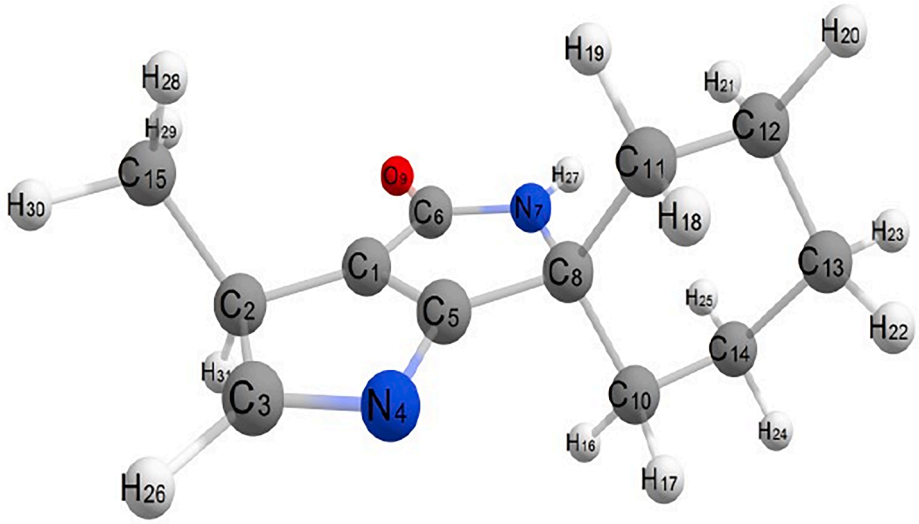

Fig. 4. Optimized geometrical structure of compound(14)by using DFT calculations.

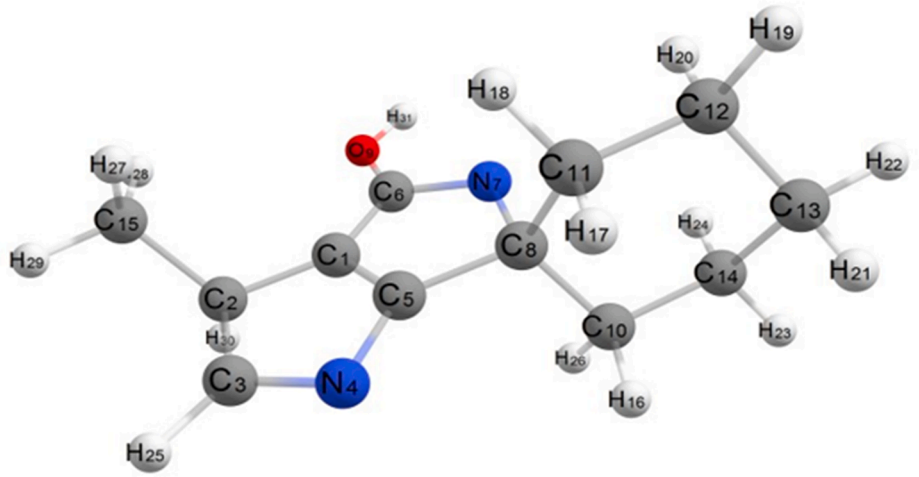

Fig. 5. Optimized geometrical structure of compound (**15**) by using DFT calculations.

(**19**), this compound is more polar than all studied compounds as given in **Table S6**, the value of dipole moment is 15.289 D, this greater valueis attributed to the presence of two carbonyl groups lying in the same side, they have the same direction, also the degree of planarity in this compound is greater than compounds (**7**, **10** and **11**). The cyclohexane ring is lying in the perpendicular plane with respect to all atoms of this compound as shown in Fig. 5 and listed dihedral angles in **Table S6**. The energy of this compound is higher thanthe energies of compounds (**7** and **10**) but lower than the energies of the compounds (**11**, **14**, and **15**), the energy of this compound is −13950.527 kcal/mol.

2.2. Molecular orbitals and frontier

Molecular orbitals also play an important role in the electric properties, as well as in UV–vis [72]. An electronic system with smaller values of HOMO-LUMO gap should be more reactive than one having a greater energy gap [73]. The energy gap is closely associated with the reactivity and stability of the executed compounds and shows the nature of the compound with low kinetic stability and slightly high chemical reactivity. On the other hand, the adjacent orbitals are often closely spaced in the frontier region. The energy gap, ΔE of the studied compounds varied between 0.138 for Compound (**10**) which more reactive, and 0.204 eV for compound (**14**) which less reactive, so electron movement between these orbitals could be easily occurred by decreasing the value of energy gap,so that there is a peak around 250 nm in the UV–vis spectra for all studied compounds.

The nodal properties of molecular orbitals of studied compounds in Fig. 6 are illustrative and suggest orbital delocalization, strong orbital overlap, and a low number of nodal planes. Fig. 7..

The energy difference between HOMO and LUMO (energy gap, △E) for all studied compounds varied according to the type of substitutions as shown in Table 1.

All studied compounds have relatively lower energy gaps than the compound **(15)**, which has relatively higher energy gap values, so these two compounds are less reactive. The values of η and △E(HOMO-LUMO) are given in Table 1. It is obvious that all studied compounds are soft molecules and η varied from 0.069 for compound (10) to 0.087 for compound (**15**), while the compound (14) is treated as a hard molecule, the value of η is 0.102, also the electronic transition within the soft compounds is easy as indicated from the △E. There are some quantum chemical parameters depending upon the energy values of HOMO and LUMO were calculated as global softness (S), electro negativity (χ), absolute softness (σ), chemical potential (Pi), global electrophilicity (ω), and additional electronic charge ($\triangle N_{max}$) of all studied compounds. From these values, the compound (10) is soft according to the (σ = 14.49 eV), while the compound (**14**) is treated as a hard compound (σ =

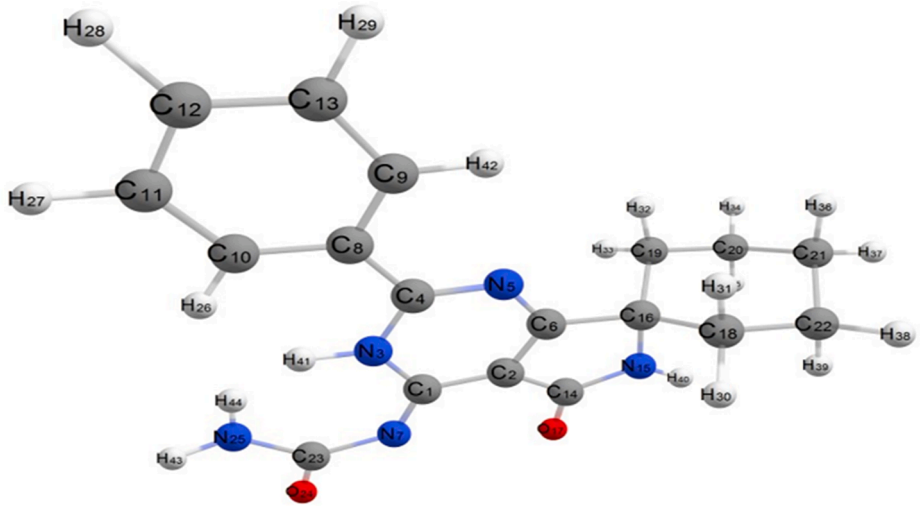

Fig. 6. Optimized geometrical structure of compound (19) by using DFT calculations.

9.804 eV).

All compounds have the same spiro system nucleus and different substations, these compounds are divided into different parts according to their composition as given in Table S7.

In compound (**7**), there are five parts, the 1st part is the spiro rings system, 2nd part is the carbonyl group, the 3rd part is the pyridine ring, the remaining 4th part is phenyl ring-1 and the 5th part is the phenyl ring-2. The electron density of HOMO of compound (**7**) is localized mainly on all atoms of the phenyl ring-2 with a percent of 59.8 %, the remaining percent is spreading over all the residual atoms. The electron density of the LUMO is also localized overall carbon atoms of Phenyl ring −2, with a percent (52.5 %) as given in Table S7.In the compound (**10**), there are four parts as given in Table S7, the electron density of the HOMO of the compound (**10**) is delocalized over all atoms, and the maximum percent is localized on the atoms of the Pyridine ring with percent 47.9 %, while in case of LUMO, the electron density delocalized over all atoms of the compound with maximum percent on pyridine ring with 31.1 %.

In the compound (**11**), there are five parts as given in Table S7, the electron density of the HOMO delocalized over all atoms with maximum percent on the atoms of Pyridine ring with percent 47.5 %, the electron density localized mainly over atoms of Pyrrole ring with percent 60.7 %. In the LUMO, the electron density delocalized over all atoms, the most percent 48.1 % is localized on the atoms of the pyrrole ring also. In compound (**15**), there are four parts, in the HOMO, the electron density is localized over atoms of the pyrrole ring with a percent of 55.4 %, and the electron density in the LUMO is delocalized overall atoms with a high percent 41.3 % on the atoms of the Pyrrole ring also. In compound (**19**), the electron density of HOMO is delocalized over all atoms of the molecule with a maximum percent localized on the diazine ring at 41.2 %, while the electron density of the LUMO is delocalized over all atoms of the molecule with a high percentage on atoms of the phenyl ring 41.0 %.

2.3. Excited state

The TD-DFT at the B3LYP level by using the G03W program proved to give an accurate description of the UV–vis. spectra [69,70]. Time-dependent density functional response theory (TD-DFT) has been recently reformulated [68] to compute discrete transition energies and oscillator strengths and has been applied to several different atoms and molecules. Bauernschmitt and Ahlrichs [72] included hybrid functionals proposed in the calculation of the excitation energies. These hybrid methods typically constitute a considerable improvement over conventional Hartree- Fock (HF) based methods. In this work, the optimized geometry was calculated and used in all subsequent calculations; the wave functions of SCF MOs were explicitly analyzed. The calculated wave functions of the different MOs reflect and suggest the fraction of the different fragments of the complex contributing to the total wave functions of different states. The results indicate that there is an extent of electron delocalization in the different molecular orbitals.

The electronic transition could be described as a mixed n → π* and π → π* transitions. The energies of HOMO and LUMO states for all studied compounds are listed in **Tables S8 and S9**. The HOMO can perform as an electron donor and the LUMO as the electron acceptor in the reaction profile.

There are seven excited states involved in the case of all studied compounds as given in Table S8 for compounds (**7**, **10**, and **11**) and in Table 8 for compounds (**14**, **15**, and **19**). In the case of compound (**7**), the first exited state results from a combination of several transitions, H-6 → L + 4(7 %), H-4 → L(10 %), H-4 → L + 1(13 %), H-4 → L + 3(11 %), H-3 → L(16 %), H-3 → L + 3(24 %), H-2 → L + 4(13 %), this excited state assigned to π-π* at 154.69 nm and 8.0151 eV. The second excited state result from the interaction between electronic configurations, which represent the π → π* transition. This is transition results from H-7 → L (11 %), H-6 → L (9 %), H-5 → L + 2 (12 %), H-1 → L + 4 (8 %), H → L + 4 (10 %) and can be observed around 158.57 nm and 7.8191 eV. The third excited state is assigned to n → π* transition, represents a transition appears at 172.36 nm and 7.1932 eV, H-7 → L + 2 (12 %), H-5 → L (8 %), H-5 → L + 1 (11 %), H-5 → L + 4(13 %), H-1 → L + 2 (24 %), H → L + 2(23 %). The fourth excited state at 181.48 nm and 6.8319 eV, results in H-1 → L + 4 (11 %), H-1 → L (9 %), H → L (13 %), and assigned to π -π*. the fifth exited state results from a combination of transitions, H-6 → L (11 %), H-2 → L + 5 (9 %), H-1 → L + 1 (12 %), H → L (8 %), this excited state assigned to π-π* at 255.16 nm and 4.8591 eV. The sixth excited state result from the interaction between electronic configurations, which represent the π → π* transition. This is transition results from H-6 → L (11 %), H-4 → L + 4 (9 %), H-4 → L + 6 (12 %), H-2 → L + 4 (8 %), H-2 → L + 5 (10 %), H → L (8 %) and can be observed around 272.50 nm and 4.5499 eV. The seventh excited state is assigned to the π → π* transition, which represents a transition that appears at 324.48 nm and 3.821 eV, H-6 → L (11 %), H-6 → L + 5 (9 %), H-2 → L (12 %), H-2 → L + 4 (8 %), H-2 → L + 6 (10 %), H → L (8 %). Also, all electronic transition configurations of the compounds (**10**) and (**11**) are given in Table S8. Also, all electronic transition configurations of compounds (**15**) and (**19**) are given in Table S9.

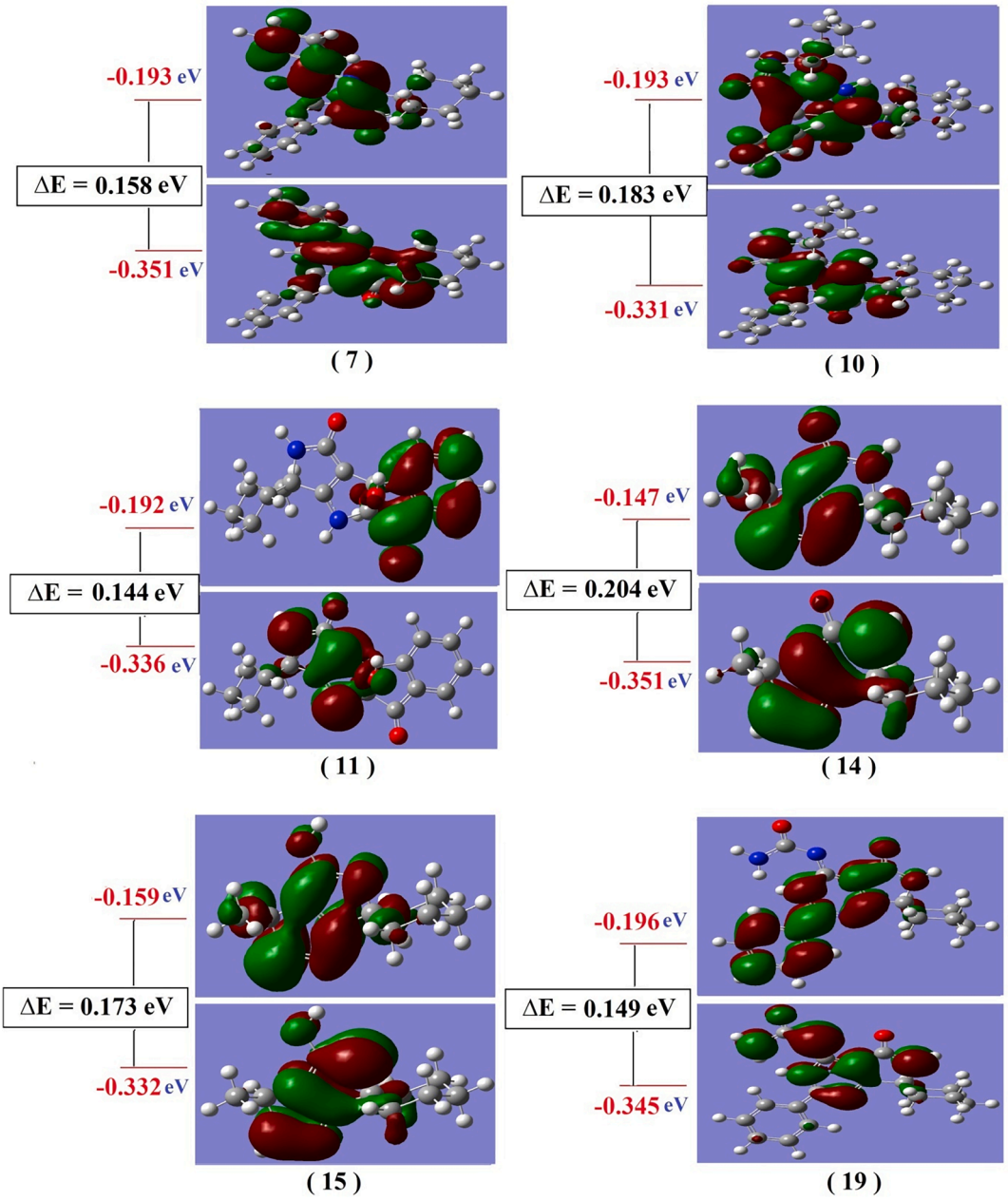

Fig. 7. Molecular orbital surfaces and energy levels of all studied compoundsby using DFT calculations.

Table 1
Calculated quantum global descriptors of the studied compounds by using DFT calculations.

Parameters	7	10	11	15	19
HOMO, H	−0.351	−0.331	−0.336	−0.332	−0.345
LUMO, L	−0.193	−0.193	−0.192	−0.159	−0.196
I	0.351	0.331	0.336	0.332	0.345
A	0.193	0.193	0.192	0.159	0.196
△E	0.158	0.138	0.144	0.173	0.149
η	0.079	0.069	0.072	0.087	0.0745
χ	0.272	0.262	0.264	0.246	0.271
σ	12.66	14.49	13.89	11.494	13.423
S	6.329	7.246	6.944	5.747	6.711
Pi	−0.272	−0.262	−0.264	−0.246	−0.271
ω	0.468	0.497	0.484	0.348	0.493
$\triangle N_{max}$	3.443	3.797	3.667	2.828	3.638

(I) is ionization energy.
(A) is an electron affinity.

2.4. anti-inflammatory and antioxidant activities

Recently, the synthesis of biologically active polycyclic compounds is gaining attention to modulate side effects of reactive oxygen species that damage biomolecules and subsequently increase the incidence of inflammation which may progress to chronic form resulting in cancer. Heterocyclic compounds can be used in a variety of biomedical applications. They can be used as antitumor agents, anti-inflammatory, anti-infective, antidiabetic, antiproliferative, antiosteoporosis, and receptor agonists[73].In this study, results revealed that the newly formed compounds exhibited both anti-inflammatory and antioxidant activities on HRBC hemolytic and membrane stabilization and DPPH scavenging percent, respectively.

Previous studies [39] reported that the mechanism of action of compounds containing pyrrole rings is due to the inhibition of COX2.

Also, many heterocyclic compounds showed a variety of biological activities like anti-inflammatory, antioxidant, anticonvulsant,

antiparasitic, and anti-HIV. Their anti-inflammatory activity may be attributed to its active centers of hydrazones (carbon and nitrogen) which monitor its properties and activities [40].

The phenyl and pyrazole derivatives have anti-inflammatory activity both in vitro and in vivo as reported [73]. They decreased lipopolysaccharide-induced inflammation in vitro. They also suppress the pro-inflammatory cytokines and prostaglandins and subsequently, they can protect dopaminergic neurons so that they can be used effectively in the treatment of Parkinson's disease. Furthermore,[75] concluded that newly synthesized pyrazole derivatives had significant COX-2 inhibitory activities more than celecoxib as a standard drug. Also, novel pyrimidine –pyridine exerted a potent cyclooxygenase inhibition and was less ulcerogenic than indomethacin [74]. In vivo anti-inflammatory activity in mice revealed that novel pyridine derivatives decreased induced sepsis by lipopolysaccharide in both lung and liver injury models. They also attenuate inducible pain and inflammation in both acetic acids induce vascular permeability and formalin-induced paw edema [75]. Another study by [76] reported that derivatives of pyrimidine can be used as potential ankyrin 1 (TRPA1) channel antagonists, consequently, they can be used effectively in the treatment of pain and inflammation.

The newly synthesized compounds have pyrrole rings that showed potent anti-inflammatory and antioxidant activities (Tables 2, 3). In this concern, previous research reported that macrocycles that consist of pyrrole rings linked through the pyrrolic 2- and 5-positions by sp3 hybridized carbon atoms showed cellular accumulation by EPR analysis of cellular fractions and high antioxidant activity in angiotensin II model of hypertension in transgenic mice expressing mitochondria-targeted catalase (m CAT), SOD2 overexpressing mice (TgSOD2) and their wild-type littermates [77]. Compounds**7**&**10**&**19** contain phenyl rings that exhibited antioxidant and anti-inflammatory activity. In this concern, previous research mentioned that compounds with phenyl rings showed a potent anti-inflammatory and antioxidant activity in DPPH protocol and acetic acid-induced writhing assay in mice, respectively [77]. Also [79] reported that newly synthesized compounds containing both phenyl and pyrazole rings showed a significant DPPH scavenging activity. They also possess central and peripheral antinociceptive responses in tail immersion tests and acetic acid-induced writhing, respectively in mice.

Newly synthesized compounds numbers **7**&**10**&**15** and **19** contain spiro rings in a percentage ranging from 13.6 to 34.5 %. Spiro compounds are of great importance in medicinal chemistry as potent antioxidants. Both naturally occurring and synthetic compounds showed significant activity by using DPPH (2,2-diphenyl-1-picrylhydrazyl), ABTS ((2, 2′-azino-bis (3-ethylbenzthiazoline-6-sulphonic acid), LPO (Lipid Peroxidation),NO(Nitric oxide),SOD(Superoxide Dismutase) and CUPRAC(Cupric ion reducing antioxidant capacity) assays[78].

Also, the presence of the carbonyl group in compounds numbers **7**&**10**&**17** resulted in their antioxidant activity. In this concern,[79] concluded that *Evolvulusalsinoides*had a significant in vitro antioxidant activity by estimating Thio barbituric acid reactive substances as it contains biologically active carbonyl molecules. In addition, [80] reported that compounds containing the carbonyl group exhibited anti-inflammatory and antioxidant properties in a turpentine oil-induced inflammation model through decreasing synthesis of NO via blocking the attachment of L. Arg in iNOS active sites.

Table 2
Hemolysis inhibition (%) of the synthesized compounds at different concentrations.

Sample concentration (µg/ml)	100	200	400	600	800	1000
Comp. 7	40.3	49.1	57.5	67.1	72.7	82.8
Comp. 10	56.8	66.5	73.6	79	87.9	95.1
Comp. 11	40.6	48.4	54.6	60.9	69.2	75.3
Comp. 18a	47.8	53.1	57	61.6	68.7	72.8
Comp. 19	47.8	55.3	67.9	75.8	83.9	91.1
Comp. 23	43.8	50.8	57.3	63.8	70.3	78.1
Standard	75.3	81.2	85.7	92.2	94.6	98

Table 3
Antioxidant assay for the tested compounds.

Compounds	Absorbance of samples	% of inhibition
7	0.665	59.8
10	0.592	64.2
11	0.311	81.2
18a	0.354	78.6
19	0.451	72.7
23	0.375	77.4

2.5. The structure activity relation (SAR)

The structure–activity relationship (SAR) on candidates exhibited a various range of potentially promising antioxidant activities., these synthesized compounds were categorized into groups of antioxidants based on the results of their biological scavenging abilities against the evaluated radicals in vitro. the presence of the carbonyl group in compounds numbers 7&10&17 resulted in their antioxidant activity.

3. Conclusion

Out of our vision, we have designed and synthesized a novel combination of compounds starting from Spiro derivative **3** was prepared quantitatively by reacting an equimolar amount of primary amine at room temperature. The compound (10) is absolute soft according to the ($\sigma = 14.49$ eV), while the compound (14) is treated as hard compounds ($\sigma = 9.804$ eV). In this study, results revealed that the newly formed compounds exhibited both anti-inflammatory and antioxidant activities on HRBC hemolytic and membrane stabilization and DPPH scavenging percent, respectively. All synthesized compound structures were elucidated via most different elemental and spectral analytical methods.

4. Materials and methods

4.1. General information

All chemicals were purchased from Sigma-Aldrich (Taufkirchen, Germany), and all solvents were purchased from El-Nasr Pharmaceutical Chemicals Company (analytical reagent grade, Egypt). 2-thiobarbituric acid was purchased from the Central Laboratory of the Health Ministry. All chemicals were used as supplied without further purification. The melting points were measured by a digital Electrothermal IA 9100 Series apparatus Cole-Parmer, Beacon Road, Stone, Staffordshire, ST15 OSA, UK) and were uncorrected. C, H, and N analyses were carried out on a PerkinElmer CHN 2400.IR spectra were recorded on FT-IR 460 PLUS (KBr disks) in the range from 4000 to 400 cm^{-1}. ^{1}H and ^{13}C NMR spectra were recorded on a Bruker 400 MHz NMR Spectrometer using tetramethylsilane (TMS) as the internal standard, chemical shifts are expressed in δ (ppm), and DMSO-d_6 was used as the solvent. The mass spectrum was carried out on a direct probe controller inlet part to a single quadrupole mass analyzer in Thermo scientific GCMS model (ISQLT) using Thermo X-Calibur software. At the Regional Center for Mycology & Biotechnology (RCMB) Al-Azhar University, Naser City, Cairo.

4.2. Synthesis

4.2.1. 4-Amino-1-azaspiro[4.5]dec-3-en-2-one (4)

A mixture of cyclohexyl amine (0.02 mol) and ethyl cyanoacetate (0.02 mol) was kept at room temperature for 24 h and the formed precipitate was filtered off, dried, and recrystallized from dilute ethanol to give compound **4**as a white powder.

m.p.120–123 °C, Yield: 96 %.IR (KBr) υ_{max}: 3300 (NH_2), 3278 (NH), 2933 (CH aliphatic), 1649 (C═O) cm^{-1}. ^1H NMR (400 MHz, DMSO-d_6) δ(ppm): 8.10 (s, 1H, NH), 8.09 (s, 2H, NH_2), 3.56 (s, 1H, pyrrole-CH), 1.75 – 1.27 (m, 10*H*, cyclohexane-H).^{13}C NMR (400 MHz, DMSO-d_6) δ(ppm): 24.48, 25.24, 25.51, 32.24, 48.38, 116.49, 160, 161.19. Anal. Calcd. for $C_9H_{14}N_2O$ (166.22): C, 65.03; H, 8.49; N, 16.85; Found: C, 65.00; H, 8.48; N, 16.85.

4.2.2. 2′,4′-Diphenyl-3′,4′-dihydrospiro[cyclohexane-1,7′-pyrrolo[3,4-b] pyridin]-5′(6′H)-one (7)

A mixture of compound **4** (0.01 mol), Benza acetophenone (0.01 mol), and triethyl amine (TEA) (4 drops) in dimethyl formamide (DMF) (15 ml) was heated under reflux for 5 h. The reaction mixture was acidified with HCl the precipitate formed was filtered off, dried, and recrystallized from ethanol to give compound **7** as a white powder.

m.p:180 °C, Yield:93 %.IR (KBr) υ_{max}: 3301 (NH), 2929 (CH aliphatic), 1677 (C═O) cm^{-1}.^1H NMR (400 MHz, DMSO-d_6) δ (ppm): 8.11 (s, 1H, NH), 8.09 – 7.18 (m, 10*H*, 2Ph-H), 3.48 d, 2H, pyridine-CH_2), 3.97, 1H, pyridine-CH), 1.64 – 1.06 (m, 5H, cyclohexane-H).^{13}C NMR (400 MHz, DMSO-d_6) δ (ppm): 24.12, 25.11, 31.90, 41.31, 43.86, 48.38, 127.23, 127.99, 128.16, 128.44, 128.85, 133.45, 136.46, 139.64, 139.73, 162.70, 162.78, 197.06. Anal. Calcd. for $C_{24}H_{24}N_2O$ (356.47), C, 80.87; H, 6.79; N, 7.86; Found: C, 80.86; H, 6.79; N, 7.87.

4.2.3. 8′-Phenyl-4′,8′-dihydrodispiro[cyclohexane-1,3′-dipyrrolo[3,4-b:3′,4′-e] pyridine-5′,1′′-cyclohexane]-1′,7′(2′ H,6′ H)-dione (10)

A mixture of compound **4** (0.01 mol), benzaldehyde (0.01 mol), and TEA (4 drops) in ethanol (20 ml) was heated under reflux for an hour. the precipitate formed after concentration was filtered off, dried, and recrystallized from hot ethanol to give compound **10** as white crystals.

m.p: 150 °C, Yield: 79.5 %. IR (KBr) υ_{max}: 3350, 3289 (NH), 2927 (CH aliphatic), 1647 (C═O), 1605 (C═N) cm^{-1}.^1H NMR (400 MHz, DMSO-d_6) δ (ppm): 8.25 (s, 2H, 2NH), 8.23 (s,1H, NH), 7.24–7.94 (m, 5H, Ph-H), 4.35 (s, 1H, pyridine-CH), 1.05 – 1.81 (m, 20H, cyclohexane-H).^{13}C NMR (400 MHz, DMSO-d_6) δ (ppm): 24.88, 32.10, 43.04, 47.70, 49.17, 107.25, 128.17, 129.35, 132,33, 134.37, 161.36, 161.44.Anal. Calcd. for $C_{25}H_{29}N_3O_2$ (403.53): C, 74.41; H, 7.24; N, 10.41; Found: C, 74.41; H, 7.24; N, 10.40.

4.2.4. 4a′,9b′-Dihydroxy-4′,4a′-dihydrospiro[cyclohexane-1,3′-indeno [2,1-b] pyrrolo[3,4-d] pyrrole]-1′,5′(2′H,9b′H)-dione (11)

A mixture of compound **4** (0.005 mol) and ninhydrin (0.005 mol) in ethanol (15 ml) was stirred at room temperature for 2 h. The precipitate formed after concentration was filtered off, dried, and recrystallized from dilute ethanol to give compound **11** as a violet powder.

m.p: 220 °C, Yield:92 %.IR (KBr) υ_{max}: 3350 (OH), 2932 (CH aliphatic), 1711 (C═O) cm ^{1}. ^1H NMR (400 MHz, DMSO-d_6) δ(ppm): 10.52 (s, 1H, OH), 8.64 (s, 2H, 2NH), 7.41 – 7.97 (m, 4H, Ar-H), 3.85 (s, 1H, OH), 1.82 – 1.00 (m, 10*H*, cyclohexane-H).^{13}C NMR (400 MHz, DMSO-d_6) δ(ppm): 25.37, 28.47, 32.11, 41.20, 61.90, 91.82, 100.48, 111.07, 111.64, 123.15, 125.95, 132.63, 136.97, 147.86, 167.26, 168.50. Anal. Calcd. for $C_{18}H_{18}N_2O_4$ (326.35): C, 66.25; H, 5.56; N, 8.58; Found: C, 66.25; H, 5.55; N, 8.57.

4.2.5. 3′-Methyl-3′H-spiro[cyclohexane-1,6′-pyrrolo[3,4-b] pyrrol]-4′-ol (15)

A mixture of compound **4** (0.003 mol), maleic anhydride (0.003 mol), and TEA (3 drops) in DMF (10 ml) was heated under reflux for 3 h. The formed precipitate after acidification with HCl, was filtered off, dried, and recrystallized from dilute ethanol to give compound **15**as white crystals.

m.p: 190 °C, Yield: 45 %.IR (KBr) υ_{max}: 3350 (OH), 2933 (CH aliphatic), cm ^{1}. ^1H NMR (400 MHz, DMSO-d_6) δ (ppm): 8.10 (s,1H, العفـروض OH), 8.08 (d, 1H, pyrrole-CH), 3.56 (m, 1H, pyrrole-CH), 1.75 – 1.24 (m, 13H, cyclohexane-H + pyrrole-CH_3). Anal. Calcd. for $C_{12}H_{16}N_2O$ (204.27): C, 70.56; H, 7.90; N, 13.71; Found: C, 70.57; H, 7.90; N, 13.70.

4.2.6. 2′- Phenyl-4′-thioxo-3′,4′-dihydrospiro[cyclohexane-1,7′-pyrrolo [3,4-d] pyrimidin]-5′(6′H)-one (18a) and 2′-(thiophen-3-yl)-4′-thioxo-3′,4′-dihydrospiro[cyclohexane-1,7′-pyrrolo[3,4-d]pyrimidine]-5′(6′H)-one (18b)General method:

Amixture of compound **4** (0.0125 mol), aroyl isothiocyanate (prepared by refluxing benzoyl chloride or thiophene-2-carbonyl chloride (0.0125) with NH_4SCN (0.0125) in dioxane for 15 min.) in dioxane (20 ml) was heated under reflux for 2hr. The precipitate formed after acidification with acetic acid and concentration was filtered off, dried, and recrystallized from dilute ethanol to give compounds**18a, b.**

4.2.7. Compound (18a)

as white crystals.m.p: 100 °C, Yield: 86.4 %. IR (KBr) υ_{max}: 3278 (NH), 2933 (CH aliphatic), 1650 (C═O) cm ^{1}. ^1H NMR (400 MHz, DMSO-d_6) δ(ppm): 9.85 (s, 1H, NH), 9.55 (s, 1H, NH), 8.10 – 7.48 (m, 5H, Ph-H), 1.75 – 1.21(m, 10*H*, cyclohexane-H).^{13}C NMR (400 MHz, DMSO-d_6) δ(ppm): 24.32, 25.09, 32.11, 48.15, 116.33, 128.40, 128.58, 132.27, 132.98, 160.96, 167.80, 182.08.Anal. Calcd. for $C_{17}H_{17}N_3OS$ (311.40): C, 65.57; H, 5.50; N, 13.49; Found: C, 65.56; H, 5.50; N, 13.48.

4.2.8. Compound (18b)

as yellowish crystals. m.p: 110 °C, Yield: 80.5 %. IR (KBr) υ_{max}: 3278 (NH), 2933 (CH aliphatic), 1650 (C═O) cm ^{1}. ^1H NMR (400 MHz, DMSO-d_6) δ (ppm): 9.72 (s, 1H, NH), 9.52 (s, 1H,NH), 8.00 – 7.20 (m, 3H, thiophene-H), 1.75 – 1.11 (m, 10*H*, cyclohexane-H). ^{13}C NMR (400 MHz, DMSO-d_6) δ(ppm): 24.33, 25.09, 32.11, 48.16, 116.34, 128.68, 132.44, 135.06, 136.95, 160.96, 161.69, 181.75.Anal. Calcd. for $C_{15}H_{15}N_3OS_2$ (317.43): C, 56.76; H, 4.76; N, 13.24; Found: C, 56.75; H, 4.75; N, 13.23.

*4.2.9. Z)-1-(5′-oxo-2′-phenyl-5′,6′-dihydrospiro[cyclohexane-1,7′-pyrrolo [3,4-d]pyrimidin]-4′(3′H)-ylidene)urea **(19)***

A mixture of compound **18a** (0.005 mol), urea (0.005 mol), and TEA (3 drops) in butanol (10 ml) was heated under reflux for 3hr. The precipitate formed after acidification with acetic acid was filtered off, dried, and recrystallized from dilute ethanol to give compound **19** as white crystals.

m.p: 150 °C, Yield: 89 %. IR (KBr) υ_{max}: 3300 (NH), 3220, 3146 (NH_2), 1676 (C═O) cm^{-1}. ^1H NMR (400 MHz, DMSO-d_6) δ(ppm): 11.23 (s, 1H, NH), 9.85 (s, 1H, NH), 9.55 (s, 2H, NH_2), 7.93 – 7.48 (m, 5H, Ph-H), 1.75 – 1.11 (m, 10*H*, cyclohexane-H). ^{13}C NMR (400 MHz, DMSO-d_6) δ(ppm): 24.13, 25.37, 32.11, 48.17, 116.35, 128.42, 128.58, 132.28, 133.00, 160.98, 167.81, 182.09.Anal. Calcd. for $C_{18}H_{19}N_5O_2$ (337.38): C, 64.08; H, 5.68; N, 20.76; Found: C, 64.07; H, 5.67; N, 20.75.

4.2.10. 10′-phenyl-5′,10′-dihydro-1′H,9′H-dispiro[cyclohexane-1,4′-pyrido[2,3-d:5,6-d′] dipyridazine-6′,1′′-cyclohexane]-1′,9′-dione (23)

A mixture of compound **10** (0.02 mol) and hydrazine hydrate (0.02 mol) in DMF (10 ml) was heated under reflux for 6 h. The precipitate formed after acidification with acetic acid was filtered off, dried, and recrystallized from hot ethanol to give compound **23** as white crystals.

m.p: 150 ^{0}C, Yield: %75. IR (KBr) υ_{max}: 3293 (NH), 2935 (CH aliphatic), 1647 (C═O) cm ^{1}. ^1H NMR (400 MHz, DMSO-d_6) δ (ppm): 8.37 (s, 1H, exchangeable with D_2O, NH), 7.57 – 7.22 (m, 5H, Ph-H), 4.33 (s, 1H, pyridine-C<u>H</u>-Ph), 1.64 – 1.13 (m, 20H, cyclohexane-H). Anal. Calcd. for $C_{25}H_{27}N_5O_2$ (429.52): C, 69.91; H, 6.34; N, 16.31; Found: C, 69.91; H, 6.33; N, 16.31.

4.2.11. 4′,10′-dimethyl-14′-phenyl-7′,14′-dihydro-2′H,12′H-dispiro [cyclohexane-1,6′-pyrido[3,2-a:5,6-a′] diindolizine-8′,1′′-cyclohexane]-2′,12′-dione (25)

A mixture of compound **10** (0.02 mol), Acetyl Acetone (0.02 mol), and TEA (4 drops) in DMF (10 ml) was heated under reflux for 6 h. The precipitate formed after acidification with acetic acid was filtered off,

dried, and recrystallized from dilute ethanol to give compound **25** as white crystals.m.p: 110 ^{0}C, Yield:79 %.IR (KBr) υ_{max}: 3278 (NH), 3087 (CH aromatic), 2933 (CH aliphatic), 1649 (C═O) cm^{-1} 1640 (C═C–C═O). ^{1}H NMR (400 MHz, DMSO-d_6) δ (ppm): 8.10 (s, 1H, NH), 7.30 – 7.25 (m, 9H, Ph-H + pyridine olefinic CH), 3.56 (s, 1H, pyridine-CH-Ph), 1.75 – 1.24 (m, 26H, cyclohexane-H + pyridine-CH_3). Anal. Calcd. for $C_{35}H_{37}N_3O_2$ (531.70): C, 79.06; H, 7.01; N, 7.90; Found: C, 79.05; H, 7.00; N, 7.89.

5. Computational details

5.1. Computational method

The geometric parameters and energies were computed by density functional theory at the B3LYP/CEP-31G level of theory, using the GAUSSIAN 98 W package of the programs [53], on geometries that were optimized at the CEP-31G basis set. The high basis set was chosen to detect the energies at a highly accurate level. The atomic charges were computed using the natural atomic orbital populations. The B3LYP is the keyword for the hybrid functional [54], which is a linear combination of the gradient functionals proposed by Becke [55] and Lee, Yang, and Parr [56], together with the Hartree-Fock local exchange function [57].

5.2. anti-inflammatory activity

Anti-inflammatory activity of the newly synthesized compounds by using membrane stabilization test [81–84].

5.3. Preparation of erythrocyte suspension:

Fresh whole blood (3 ml) collected from healthy volunteers into heparinized tubes was centrifuged at 3000 rpm for 10 min. A volume of normal saline equivalent to thatof the supernatant was used to dissolve the red blood pellets. The volume of the dissolved red blood pellets obtained was measured and reconstituted as a 40 % v/v suspension with isotonic buffer solution (10 mM sodium phosphate buffer,PBS, pH 7.4). The buffer (PBS) solution contained 0.2 g of NaH_2PO_4, 1.15 g of Na_2HPO_4, and 9 g of NaCl in 1 L of distilled water. The reconstituted red blood cells (resuspended supernatant) were used as such.

5.4. Hypotonicity-induced hemolysis:

Samples used in this test were dissolved in distilled water (hypotonic solution). The hypotonic solution (5 ml) containing graded doses of the samples (100, 200, 400, 600, 800, and 1000 μg/ml) was put into duplicate pairs (per dose) of the centrifuge tubes. Isotonic solution (5 ml) containing graded doses of the samples (100 – 1000 μg/ml) was also put into duplicate pairs (per dose) of the centrifuge tubes. Control tubes contained 5 ml of the vehicle (distilled water) and 5 ml of 200 μg/ml of indomethacin respectively. Erythrocyte suspension (0.1 ml) was added to each of the tubes and mixed gently. The mixtures were incubated for 1 hr at room temperature (37 °C), and afterward, centrifuged for 3 min at 1300 g. Absorbance (OD) of the hemoglobin content of the supernatant was estimated at 540 nm using Spectronic (Milton Roy) spectrophotometer. The percentage of hemolysis was calculated by assuming the hemolysis produced in the presence of distilled water as 100 %. The percent of hemolysis inhibition by the samples was calculated as the following:

% Inhibition of hemolysis = 1-((OD2-OD1)/ (OD3-OD1)) *100.

Where OD1 = absorbance of the test sample in an isotonic solution.

OD2 = absorbance of the test sample in a hypotonic solution.

OD3 = absorbance of control sample in a hypotonic solution.

6. Antioxidant activity

6.1. Evaluation of antioxidant activity by DPPH radical scavenging method

Free radical scavenging activity of different samples was measured by 1, 1- diphenyl-2-picryl hydrazyl (DPPH). In brief, 0.1 mM solution of DPPH in ethanol was prepared. This solution (1 ml) was added to 3 ml. of different samples in ethanol at different concentration (3.9, 7.8, 15.62, 31.25, 62.5, 125, 250, 500, 1000 μg/ml). Here, only those samples used which are soluble in ethanol and their various concentrations were prepared by dilution method. The mixture was shaken vigorously and allowed to stand at room temperature for 30 min and then the absorbance was measured at 517 nm by using a spectrophotometer (UV–vis Milton Roy). The used reference standard compound was ascorbic acid, and the experiment was carried out in triplicate. The IC_{50} value of the sample, which is the concentration of sample required to inhibit 50 % of the DPPH free radical, was calculated using the Log dose inhibition curve. The lower absorbance of the reaction mixture indicated higher free radical activity. The percent DPPH.

The scavenging effect was calculated by using the following equation:

DPPH scavenging effect (%) or.

Percent inhibition = A0 - A1 / A0 × 100.

Where A0 was the absorbance of the control reaction.

A1 was the absorbance in presence of a test or standard sample.

Declaration of Competing Interest

The authors declare that they have no known competing financial interests or personal relationships that could have appeared to influence the work reported in this paper.

Data availability

The authors do not have permission to share data.

Appendix A. Supplementary material

Supplementary material to this article can be found online at https://doi.org/10.1016/j.bioorg.2022.106280.

References:

[1] A. Mermer, T. Keles, Y. Sirin, Recent studies of nitrogen containing heterocyclic compounds as novel antiviral agents: a review, Bioorg Chem 114 (2021), 105076, https://doi.org/10.1016/j. bioorg.2021.105076.

[2] I. Natsutani, R. Iwata, Y. Yamai, K. Ishida, Y. Nagaoka, T. Sumiyoshi, Design, synthesis, and evaluations of spiro-fused benzoxaborin derivatives as novel boron-containing compounds, Chem. Biol. Drug Des. 93 (2019) 657–665, https://doi.org/10.1111/cbdd.13496.

[3] M. Moghaddam-Manesh, D. Ghazanfari, E. Sheikhhosseini, M. Akhgar, MgO-Nanoparticle-Catalyzed Synthesis and Evaluation of Antimicrobial and Antioxidant Activity of New Multi-Ring Compounds Containing Spiro[indoline-3,4′-[1,3] dithiine], ChemistrySelect 4 (31) (2019) 9247–9251.

[4] M.M.K. Amer, M.A. Aziz, W.S. Shehab, M.H. Abdellattif, S.M. Mouneir, Recent advances in chemistry and pharmacological aspects of 2-pyridone scaffolds, Journal of Saudi Chemical Society 25 (6) (2021) 101259.

[5] S. Balasubramanian, C. Ramalingan, G. Aridoss, S. Kabilan, Synthesis, and study of antibacterial and antifungal activities of novel 8-methyl-7,9-diaryl1,2,4,8-tetraa-zaspiro [4.5] decan-3-thiones, Eur. J. Med. Chem. 40 (2005) 694–700, https://doi.org/10.1016/j.ejmech.2005.02.001.

[6] J.-L. Reymond, M. Awale, Exploring chemical space for drug discovery using the chemical universe database, ACS Chem Neurosci 3 (9) (2012) 649–657.

[7] M.J. James, P. O'Brien, R.J.K. Taylor, W.P. Unsworth, Synthesis of Spirocyclic Indolenines, Chem Eur J 22 (9) (2016) 2856–2881.

[8] P.N. Kalaria, S.C. Karad, D.K. Raval, A review on diverse heterocyclic compounds as the privileged scaffolds in antimalarial drug discovery, Eur J Med Chem 158 (2018) 917–936.

[9] W. Li, S.J. Zhao, F. Gao, Z.S. Lv, J.Y. Tu, Z. Xu, Synthesis and in vitro anti-tumor, anti-mycobacterial and anti-HIV activities of diethylene-glycol-tethered bis-isatin derivatives, Chem Sel 3 (2018) 10250–10254.

[10] X. Zhao, S.T. Chaudhry, J. Mei, Heterocyclic building blocks for organic semiconductors. Heterocyclic chemistry in the 21st Century a Tribute to Alan Katritzky. 121 (2017) 133–171.
[11] T.A. Khattab, M.A. Rehan, Egypt J Chem 61 (2018) 989–1018.
[12] Lamberth C, Dinges J (2012) Bioactive heterocyclic compound classes: agrochemicals. Wiley, KGaA.
[13] R. Ramachandran, M. Rani, S. Senthan, Y.T. Jeong, S. Kabilan, Synthesis, spectral, crystal structure and in vitro antimicrobial evaluation of imidazole/benzotriazole substituted piperidin-4-one derivatives, Eur. J. Med. Chem. 46 (2011) 1926–1934, https://doi.org/10.1016/j.ejmech.2011.02.036.
[14] A. Sethukumar, P.S. Anand, C.U. Kumar, B.A. Prakasam, Synthesis, stereochemical and biological studies of some N-cyclohexylcarbamoyl -2,6-diarylpiperidin4-ones, J. Mol. Struct. 1130 (2017) 352–362, https://doi.org/10.1016/j.molstruc.2016.10.035.
[15] G. Aridoss, S. Balasubramanian, P. Parthiban, S. Kabilan, Synthesis and NMR spectral studies of N-chloroacetyl-2,6-diarylpiperidin-4-ones, Spectrochim. Acta Part A Mol, Biomol. Spectrosc. 68 (2007) 1153–1163, https://doi.org/10.1016/j.saa.2007.01.013.
[16] J. Chakkaravarthy, G. Muthukumaran, K. Pandiarajan, Conformational study of some N-acyl-2r,6c-diphenylpiperidin-4-one oximes using NMR spectra, J. Mol. Struct. 889 (2008) 297–307 https://doi.org/, doi: 10.1016/j.molstruc.2008.02.008.
[17] D. Osman, A. Cooke, T.R. Young, E. Deery, N.J. Robinson, et al., The requirement for cobalt in vitamin B12: a paradigm for protein metalation, BiochimBiophys Acta Mol Cell Res 1868 (2021), 118896, https://doi.org/10.1016/j.bbamcr.2020.
[18] M.L. Santos, M. D'Ambrosio, A.P. Rodrigo, A.J. Parola, P.M. Costa, A transcriptomic approach to the metabolism of tetrapyrrolic photosensitizers in a marine annelid, Molecules 26 (2021) 3924, https://doi.org/10.3390/molecules26133924.
[19] D.D. Haines, A. Tosaki, Heme degradation in pathophysiology of and counter measures to infammation-associated disease, Int J Mol Sci 21 (2020) 9698, https://doi.org/10.3390/ijms21249698.
[20] H.L. Bonkovsky, N. Dixon, S. Rudnick, Pathogenesis and clinical features of the acute hepatic porphyrias (AHPs), Mol Genet Metab 128 (2019) 213–218, https://doi.org/10.1016/j.ymgme. 2019.03.002.
[21] S. Lin, E. McCauley, N. Lorig-Roach, K. Tenney, C. Naphen, A.-M. Yang, T. Johnson, T. Hernadez, R. Rattan, F. Valeriote, P. Crews, Another look at pyrroloiminoquinone alkaloids-perspectives on their therapeutic potential from known structures and semisynthetic analogues, Mar Drugs 15 (4) (2017) 98.
[22] A. Cipres, D.P. O'Malley, K.e. Li, D. Finlay, P.S. Baran, K. Vuori, Sceptrin, a marine natural compound, inhibits cell motility in a variety of cancer cell lines, ACS Chem Biol 5 (2) (2010) 195–202.
[23] K. Vijay, T.S. Devi, K.K. Sree, A.M. Elgorban, P. Kumar, et al., In vitro screening and in silico prediction of antifungal metabolites from rhizobacterium Achromobacterkerstersii JKP9, Arch Microbiol 20 (2020) 2855–2864, https://doi.org/10.1007/s00203-020-01982-0.
[24] H.Y. Xiang, J.Y. Chen, X.J. Huan, Y. Chen, Z.B. Gao, et al., Identifcation of 2-substituted pyrrolo[1,2-b]pyridazine derivatives as new PARP-1 inhibitors Bioorg, Med. Chem. Lett 31 (2021), 127710, https://doi.org/10.1016/j.bmcl.2020.127710.
[25] D.A. Mendonça, M. Bakker, C. Cruz-Oliveira, V. Neves, M.A. Jimenez, et al., Penetrating the blood-brain barrier with new peptide-porphyrin conjugates having anti-hiv activity, Bioconjug Chem 32 (2021) 1067–1077, https://doi.org/10.1021/acs.bioconjchem.
[26] S. Krishnamurthy, H. Yoda, K. Hiraoka, T. Inoue, J. Lin, Y. Shinozaki, T. Watanabe, N. Koshikawa, A. Takatori, H. Nagase, Targeting the mutant PIK3CA gene by DNA-alkylating pyrroleimidazole polyamide in cervical cancer, Cancer Sci 112 (3) (2021) 1141–1149.
[27] B.M. Cawrse, N.M. Robinson, N.C. Lee, G.M. Wilson, K.L. Seley-Radtke, Structural and biological investigations for a series of n-5 substituted pyrrolo [3,2-d] pyrimidines as potential anticancer therapeutics, Molecules 24 (2019) 2656, https://doi.org/10.3390/molecules24142656.
[28] U. Leone Roberti Maggiore, M. Valenzano Menada, P.L. Venturini, S. Ferrero, The potential of sunitinib as a therapy in ovarian cancer, Expert Opinion on Investigational Drugs 22 (12) (2013) 1671–1686.
[29] Lang DK, Kaur R, Arora R, Saini B, Arora S (2020) Nitrogencontaining heterocycles as anticancer agents: an overview. Anticancer Agents Med Chem 20:2150–2168. https://doi.org/10. 2174/1871520620666200705214917.
[30] A.Z. Crepeau, D.M. Treiman, Levetiracetam: a comprehensive review, Expert Review of Neurotherapeutics 10 (2) (2010) 159–171.
[31] J. Jiang, X. Li, M. Hanif, J. Zhou, D. Hu, S. Su, Z. Xie, Y. Gao, B. Yang, Y. Ma, Pyridal[2,1,3]thiadiazole as strong electron-withdrawing and less stericallyhindered acceptor for highly efficient donor–acceptor type NIR materials, J. Mater. Chem. C. 5 (2017) 11053–11058, https://doi.org/10.1039/C7TC03978F.
[32] T. Ghosh, M. Lehmann, Recent advances in heterocycle-based metal-free calamitics, J. Mater. Chem. C. 5 (2017) 12308–12337, https://doi.org/10.1039/C7TC03502K.
[33] D. Bora, A. Kaushal, N. Shankaraiah, Anticancer potential of spirocompounds in medicinal chemistry: A pentennial expedition, Eur. J. Med. Chem. 215 (2021), 113263, https://doi.org/10.1016/j.ejmech.2021.113263.
[34] L.M.T. Frija, A.J.L. Pombeiro, M.N. Kopylovich, Building 1,2,4-Thiadiazole: Ten Years of Progress, European J. Org. Chem. 2017 (2017) 2670–2682 https://doi.org/, doi:10.1002/ejoc.201601642.
[35] H. Fischer and H. Orth, Die Chemie des Pyrrols, AkademischeVerlagsgesellschaftmbh., Leipzig (1934).
[36] R.A. Jones, Pyrroles: The Synthesis and the Physical and Chemical Aspects of the Pyrrole ring, Wiley-Interscience, 1990.
[37] AbdEl-Azim, MHM, Aziz, MA, Mouneir, SM, EL-Farargy, AF, Shehab, WS. Ecofriendly synthesis of pyrano[2,3-*d*]pyrimidine derivatives and related heterocycles with anti-inflammatory activities. *Arch Pharm*. 2020; 353:e2000084. https://doi.org/10.1002/ardp.202000084.
[38] A. Thurkauf, J. Yuan, N. Chen, et al., J. Med. Chem. 38 (25) (1995) 4950–4952.
[39] W.W. Wilkerson, R.A. Copeland, M. Covington, J.M. Trzaskos, J. Med. Chem. 38 (20) (1995) 3895–3901.
[40] A. Kajal, S. Bala, N. Sharma, et al., Int. J. Med. Chem. 2014 (2014).
[41] K.N. de Oliveira, P. Costa, J.R. Santin, et al., Bioorg. Med. Chem. 19 (14) (2011) 4295–4306.
[42] C.M. Leal, S.L. Pereira, A.E. Kümmerle, et al., Eur. J. Med. Chem. 55 (2012) 49–57.
[43] L. Yurttaþ, Y. Özkay, Z.A. Kaplancýklý, et al., J. Enzyme Inhib. Med. Chem. 28 (4) (2013) 830–835.
[44] O.O. Ajani, C.A. Obafemi, O.C. Nwinyi, D.A. Akinpelu, Bioorg. Med. Chem. 18 (1) (2010) 214–221.
[45] J.V. Ragavendran, D. Sriram, S.K. Patel, et al., Eur. J. Med. Chem. 42 (2) (2007) 146–151.
[46] J.R. Dimmock, S.C. Vashishtha, J.P. Stables, Eur. J. Med. Chem. 35 (2) (2000) 241–248.
[47] S.I. Alqasoumi, M.M. Ghorab, Z.H. Ismail, et al., Arzneimittelforschung 59 (12) (2009) 666–671.
[48] A.A. El-Tombary, S.A.M. El-Hawash, Med. Chem. 10 (5) (2014) 521–532.
[49] M.A. Aziz, W.S. Shehab, A.A. Al-Karmalawy, A.F. El-Farargy, M.H. Abdellattif, Design, Synthesis, Biological Evaluation, 2D-QSAR Modeling, and Molecular Docking Studies of Novel 1 H-3-Indolyl Derivatives as Significant Antioxidants, International journal of molecular sciences 22 (19) (2021) 10396.
[50] P.D. MacLean, E.E. Chapman, S.L. Dobrowolski, et al., J. Org. Chem. 73 (17) (2008) 6623–6635.
[51] J.D. Bhosale, A.R. Shirolkar, U.D. Pete, et al., J. Pharm. Res. 7 (7) (2013) 582–587.
[52] A. Khalilpour, S. Asghari, Med. Chem. Res. 27 (1) (2018) 15–22.
[53] Gaussian 98, Revision A.6, M. J. Frisch, G. W. Trucks, H. B. Schlegel, G. E. Scuseria, M.A.Robb, J.R.Cheeseman, V.G. Zakrzewski, J.A. Montgomery, R.E.Stratmann, J.C. Burant, S.Dapprich, J.M.Millam, A.D.Daniels, K.N. Kudin, M.C. Strain, O. Farkas, J. Tomasi, V. Barone, M. Cossi, R. Cammi, B.Mennucci, C. Pomelli, C. Adamo, S. Clifford, J. Ochterski, G. A. Petersson, P. Y. Ayala, Q. Cui, K. Morokuma, D. K. Malick, A.D.Rabuck, K. Raghavachari, J.B. Foresman, J.Cioslowski, J.V.Ortiz, B.B. Stefanov, G.Liu, A.Liashenko, P.Piskorz, I. Komaromi, R.Gomperts,R. L. Martin, D. J. Fox, T. Keith, M. A. Al-Laham, C. Y. Peng, A. Nanayakkara, C. Gonzalez, M. Challacombe, P. M. W. Gill, B. Johnson, W. Chen, M. W. Wong, J. L.Andres, C. Gonzalez, M. Head-Gordon, E. S. Replogle, and J. A. Pople, Gaussian, Inc., Pittsburgh PA, 1998.
[54] W. Kohn, L.J. Sham, Phys. Rev A. 140 (1965) 1133.
[55] A.D. Becke, Phys. Rev. A. 38 (1988) 3098.
[56] C. Lee, W. Yang, R.G. Parr, Phys. Rev B 37 (1988).
[57] R. L. Flurry Jr., Molecular Orbital Theory of Bonding in Organic Molecules, Marcel Dekker, New York, 1968.
[58] S. Top, J. Tang, A. Vessieres, C. Carrez, C. Provot, G. Jaouen, Chem. Commun. (J. Chem. Soc. Sect. D) (1996) 955–956.
[60] I. Turel, L. Golic, P. Bukovec, M. Gubina, Journal of Inorganic Biochemistry 71 (1998) 53.
[61] M. Becka, M. Vilkova, M. Soral, I. Potocnak, M. Breza, T. Beres, J. Imrich, Journal of Molecular Structure 1154 (2018) 152–164.
[62] I. Turel, P. Bukovec, M. Quiros, Int. J. Pharm. 152 (1997) 59.
[63] E. Aktan, B. Babür, N. Seferoglu, B. Çatıkkas, F.B. Kaynak, Z. Seferoglu, Journal of Molecular Structure 1145 (2017) 152–159.
[64] J.G. Haasnoot, Coord. Chem. Rev. 200 (2000) 131.
[65] I. Fleming, Frontier Orbitals and Organic Chemical Reactions, Wiley, London, 1976.
[66] R. Kurtaran, S. Odabasoglu, A. Azizoglu, H. Kara, O. Atakol, Polyhedron 26 (2007) 5069–5074.
[67] K. Krogmann, Z. Anorg, Allg. Chem. 346 (1966) 188–202.
[68] I. Ciofini, P.P. Laine, F. Bedioui, C. Admo, J. Am. Chem. Soc. 126 (2004) 10763.
[69] I. Ciofini, C. Daul, C, J, Adamo. *J. Phys. Chem. A* **2003**, *107, 11182.49*.
[70] F. M. Casida, In Recent Advances in Density Functional Methods, part 1; Chong, D. P., Eds.; World Scientific: Singapore, **1995**.
[71] R. Bauernschmitt, R. Ahlrichs, Chem Phys Lett 256 (1996) 454.
[72] Ana Donaire-Arias , Ana Maria Montagut, Raimon Puig de la Bellacasa , Roger Estrada-Tejedor, Jordi Teixidó and José I. Borrell. 1H-Pyrazolo[3,4-b]pyridines: Synthesis and Biomedical Applications.Molecules 2022, 27, 2237. https://doi.org/10.3390/molecules27072237.
[73] W. S. Shehab, A. F. EL-Farargy, A. O. Abdelhamid, M. A. Aziz, Synthesis and biological application of pyranopyrimidine derivatives catalyzed by efficient nanoparticles and their nucleoside analogues. *Synth. Commun.* 2019, **49**, 3560. https://doi.org/10.1080/00397911.2019.1679538.
[74] W.S. Shehab, M.H. Abdellattif, S.M. Mouneir, Heterocyclization of polarized system: synthesis, antioxidant and anti-inflammatory 4-(pyridin-3-yl)-6-(thiophen-2-yl) pyrimidine-2-thiol derivatives, Chem. Cent. J. 12 (2018) 68, https://doi.org/10.1186/s13065-018-0437-y.
[75] Mohamed A Abdelgawad , Rania B Bakr , Amany A Azouz .Novel pyrimidine-pyridine hybrids: Synthesis, cyclooxygenase inhibition, anti-inflammatory activity and ulcerogenic liability.Bioorg chem. 2018 77:339-348. DOI: 10.1016/j.bioorg.2018.01.028.
[76] W. H. El-Shwiniy, W. S. Shehab, W. A. Zordok, , Spectral, thermal, DFT calculations, anticancer and antimicrobial studies for bivalent manganese

complexes of pyrano [2, 3-d] pyrimidine derivatives. *J. Mol. Struct.* 2020, **1199**, 126993.

[77] Baraldi, P.G.; Romagnoli, R.; Saponaro, G.; Tabrizi, M.A.; Baraldi, S.; Pedretti, P.; Fusi, C.; Nassini, R.;Materazzi, S.; Geppetti, P.; et al. 7-Substituted-pyrrolo[3,2-d] pyrimidine-2,4-dione derivatives as antagonists of the transient receptor potential ankyrin 1 (TRPA1) channel: A promising approach for treating pain and inflammation. Bioorg. Med. Chem. 2012, 20, 1690–1698.https://doi.org/10.1016/j.bmc.2012.01.020.

[78] Dikalov SI, Dikalova AE, Morozov DA, Kirilyuk IA. Cellular accumulation and antioxidant activity of acetoxymethoxycarbonyl pyrrolidine nitroxides. Free Radic Res. 2018 Mar;52(3):339-350. doi: 10.1080/10715762.2017.1390744. Epub 2017 Nov 3. PMID: 29098905; PMCID: PMC5915311.

[79] Terence Nguema Ongone ,RedouaneAchour, Mostafa El Ghoul, Latyfa El Ouasif, Meryem El Jemli, Laila Chemlal, Yahia Cherrah, KatimAlaoui, and Amina Zellou. Analgesic and Antioxidant Activities of4-Phenyl-1,5-benzodiazepin-2-one and Its Long CarbonChains Derivatives.Journal of Chemistry, vol. 2019, Article ID 9043570, 7 pages, 2019. https://doi.org/10.1155/2019/9043570.

[80] S.A. Ali, S.M. Awad, A.M. Said, S. Mahgoub, H. Taha, N.M. Ahmed, Design, synthesis, molecular modelling and biological evaluation of novel 3-(2-naphthyl)-1-phenyl-1H-pyrazole derivatives as potent antioxidants and 15-Lipoxygenase inhibitors, J Enzyme Inhib Med Chem. 35 (1) (2020 Dec) 847–863, https://doi.org/10.1080/14756366.2020.1742116. PMID: 32216479; PMCID: PMC7170299.

[81] Karen Acosta-Quiroga, Cristian Rojas-Pena, a Luz Stella Nerio, Margarita Gutierreź and Efráın Polo-Cuadrado. Spirocyclic derivatives as antioxidants: a review.Royal society of chemistry. RSC Adv., 2021, 11, 21926. DOI: 10.1039/d1ra01170g.

[82] DuraisamyGomathia,GanesanRavikumar,ManokaranKalaiselvi, KanakasabapathiDevaki,ChandrasekarUma. Antioxidant activity and functional group analysis of *Evolvulusalsinoides*. Chinese Journal of Natural Medicines 12(11), 11, 2014, 827-832.https://doi.org/10.1016/S1875-5364(14)60124-2.

[83] B. Tiperciuc, A. Pârvu, R.d. Tamaian, C. Nastasă, I. Ionuţ, O. Oniga, New anti-inflammatory thiazolyl-carbonyl-thiosemicarbazides and thiazolyl-azoles with antioxidant properties as potential iNOS inhibitors, Arch. Pharm. Res. 36 (6) (2013 Jun) 702–714, https://doi.org/10.1007/s12272-013-0083-9.

[84] U.A. Shinde, A.S. Phadke, A.M. Nair, A.A. Mungantiwar, V.J. Dikshit, M.N. Saraf, Membrane stabilization activity- a possible mechanism of action for the anti-inflammatory activity of Cedrusdeodara wood oil, Fitoterapia 70 (1989) 251–257.

Further reading

[59] A. Siddekha, A. Nizam, M.A. Pasha, Spectrochimica Acta Part A 81 (2011) 431–440.